

Small-molecule ligands that bind the RET receptor activate neuroprotective signals independent of but modulated by co-receptor GFR α 1

Sean Jmaeff ^{1,2}, Yulia Sidorova ³, Hayley Lippiatt ¹, Pablo F. Barcelona ¹, Hinyu Nedev ¹, Lucia M. Saragovi ¹, Mark A. Hancock ⁴, Mart Saarma ³, H. Uri Saragovi ^{1,2}

¹ Lady Davis Institute - Jewish General Hospital. McGill University. Montreal, CANADA.

² Pharmacology and Therapeutics. McGill University. Montreal, CANADA.

³ Institute of Biotechnology. HiLIFE. University of Helsinki. Helsinki, FINLAND.

⁴ SPR-MS Facility, McGill University, Montreal, CANADA

of Text Pages (excluding references): 29

of Tables: 0

of Figures: 5

of References: 55

of Words in Abstract: 143

of Words in Introduction: 462

of Words in Discussion: 1512

Running title: validation of RET receptor as a druggable target

List of Abbreviations:

BSA: Bovine Serum Albumin

CHO: Chinese Hamster Ovary

CRALBP: Cellular Retinaldehyde Binding-Protein

DAPI: 4',6-diamidino-2-phenylindole

DMEM: Dulbecco's Modified Eagle's Medium

DMSO: Dimethyl sulfoxide

FBS: Fetal Bovine Serum
FGF2: Fibroblast Growth Factor 2
GDNF: Glial cell line-derived neurotrophic factor
GFR α 1: GDNF Family Receptor alpha 1
GPI: Glycosylphosphatidylinositol
INL: Inner Nuclear Layer
NCAM: Neuronal Cell Adhesion Molecule
NGF: Nerve Growth Factor
ONL: Outer Nuclear Layer
PBS: Phosphate Buffered Saline
PD: Parkinson's Disease
PFA: Paraformaldehyde
pTyr: phospho-tyrosine
RGC: Retinal Ganglion Cell Layer
RP: Retinitis Pigmentosa
RTK: Receptor Tyrosine Kinase
RU: Resonance Units
SAR: Structure-Activity Relationship
SFM: Serum-free Media
SPR: Surface Plasmon Resonance
SSC: Saline Sodium Citrate
TdT: Terminal Deoxynucleotidyl Transferase
TGF: Transforming Growth Factor
TrkA: Tropomyosin Receptor Kinase A
TUNEL: Terminal deoxynucleotidyl transferase dUTP nick end labeling

Abstract

Glial cell line-Derived Neurotrophic Factor (GDNF) binds the GFR α 1 receptor, and the GDNF–GFR α 1 complex binds to and activates the transmembrane RET tyrosine kinase to signal through intracellular Akt/Erk pathways. To dissect the GDNF–GFR α 1–RET signaling complex, agents that bind and activate RET directly and independently of GFR α 1 expression are valuable tools. In a focused naphthalenesulfonic acid library from the NCI database, we identified small molecules that are genuine ligands binding to the RET extracellular domain. These ligands activate RET tyrosine kinase and afford trophic signals irrespective of GFR α 1 co-expression. However, RET activation by these ligands is constrained by GFR α 1, likely via an allosteric mechanism that can be overcome by increasing RET ligand concentration. In a mouse model of retinitis pigmentosa, monotherapy with a small molecule RET agonist activates survival signals and reduces neuronal death significantly better than GDNF, suggesting therapeutic potential.

Significance Statement

A genuine ligand of RET receptor ectodomain was identified, which acts as an agonist. Binding and agonism are independent of a co-receptor GFR α which is required by the natural growth factor GDNF, and are selective for cells expressing RET. The lead agent protects neurons from death *in vivo*. This work validates RET receptor as a druggable therapeutic target, and provides for potential leads to evaluate in neurodegenerative states. We also report problems that arise when screening chemical libraries.

Introduction

Glial cell line-derived neurotrophic factor (Nutt, Burchiel et al.), a distant member of the TGF-beta superfamily, mediates pro-survival signaling in neuronal populations (Airaksinen and Saarma 2002, Runeberg-Roos and Saarma 2007, Ibanez 2013). Indeed, GDNF has been tested in animal models of neurodegeneration, notably Parkinson's Disease (PD), Amyotrophic Lateral Sclerosis, neuropathic pain (Boucher, Okuse et al. 2000), and eye diseases such as retinitis pigmentosa (RP) and glaucoma (McGee Sanftner, Abel et al. 2001, Gregory-Evans, Chang et al. 2009, Ohnaka, Miki et al. 2012).

In human clinical trials for PD, the therapeutic efficacy of GDNF and related factor neurturin has been controversial, with post hoc analysis showing clinically significant motor improvement (Josephy-Hernandez, Jmaeff et al. 2017, Whone, Luz et al. 2019). In part, GDNF therapy remains a challenging strategy due to the limited understanding of the physiology of its receptors, varying receptor/co-receptor expression patterns, and binding or functional interactions with other factors or matrix proteins *in vivo* (Sariola and Saarma 2003, Gash, Zhang et al. 2005, Touchard, Heiduschka et al. 2012). GDNF can bind to extracellular matrix and transmembrane heparan sulfate proteoglycans and neuronal cell adhesion molecules NCAM (Hamilton, Morrison et al. 2001, Bespalov and Saarma 2007), affecting its bioavailability (Salvatore, Ai et al. 2006). These issues could be solved using RET agonists that are not bound/trapped, and which may exhibit more favorable kinetics and avoid the need for invasive delivery methods.

GDNF binds first to the GPI-anchored GDNF Family Receptor alpha 1 (GFR α 1) receptor, and the resulting GDNF/GFR α 1 complex then activates the RET receptor tyrosine kinase (RTK). There appears to be a functional cross-regulation between RET and GFR α 1, as reported for another receptor family, the neurotrophin receptors (Ivanisevic, Banerjee et al. 2003). However, the required concomitant presence of GFR α 1 and RET receptors to activate measurable GDNF-induced signals limits biological and pharmacological studies.

For example, studies of cross-regulation are difficult, and access to receptor-specific ligands would be useful to probe this question. Moreover, the pharmacological utility of GDNF may be limited to indications where both receptors are present in the same

tissue in disease. However, there are indications where RET is expressed without GFR α 1, for example, in the retina (Brantley, Jain et al. 2008). Selective, small molecule RET agonists may provide a broader range of tissue targets and activities.

Here we report chemical biology studies to develop small molecules that selectively activate RET-pY¹⁰⁶², which activates Akt and Erk pathways leading to cell survival-promoting signals. Activity is dependent on RET-expression, but independent of GFR α 1-expression. We used these small molecules as tools to demonstrate regulation of RET by GFR α 1, a process which is likely allosteric. A RET agonist, compound 8, was used as a therapeutic lead in an animal model of retinitis pigmentosa, to validate the RET receptor as a druggable target in this disease.

Materials and Methods

Cell Lines

MG87 RET are murine MG87 fibroblasts stably transfected with RET proto-oncogene cDNA (Eketjall, Fainzilber et al. 1999), and were cultured in DMEM containing 10% FBS, 2 mM L-Glutamine, 10 mM HEPES, 100 U/ml Penicillin/Streptomycin, and 2 µg/ml puromycin. MG87 RET cells were transfected with a GFR α 1 cDNA construct containing Blasticidin resistance gene to generate the MG87 RET/GFR α 1 cell line, and were cultured in the same media with the addition of 5 µg/ml Blasticidin S. MG87 TrkA cells were transfected with human NGF receptor TrkA cDNA, and cultured in DMEM 10% FBS supplemented with 250 µg/ml G418. MG87RET/GFR α 1 cell lines were stably transfected with PathDetect Elk-1 system (Stratagene) harboring Luciferase reporter under the control of Erk activity. Cells were cultured in DMEM, 10% FBS, 15 mM HEPES pH 7.2, 100 µg/ml normocin (Invivogen), 2 µg/ml puromycin, 500 µg/ml (Sidorova, Matlik et al. 2010). Growth factors GDNF and NGF were purchased from Peprtech (catalogue 450-10, 450-01) and FGF2 from Sigma Aldrich (catalogue F0291). Cell lines were routinely tested and verified to be free of mycoplasma (Venor GeM Mycoplasma Detection Kit).

Luciferase assay

Initial screening of a chemical library was performed in MG87RET/GFR α 1 cells with luciferase reporter controlled by Erk (Sidorova, Matlik et al. 2010). 20000 cells per well were plated in 96-well plates in DMEM, 10% FBS, 15 mM HEPES pH 7.2, 100 µg/ml normocin, 1% DMSO and incubated overnight under standard conditions. Cells were treated with tested compounds dissolved in DMEM, 15 mM HEPES pH 7.2, 1% DMSO to achieve final concentration of 5 and 20 µM for 24-30 hr. Afterwards, cells were lysed with 25 µl of cell lysis buffer (Promega) per well and frozen and thawed once. Five µl of lysate was combined with 20 µl of luciferase assay reagent (Promega) on ice. Luminescence was measured using MicroBeta 2 instrument (PerkinElmer) twice. Results of the second run were used for analysis.

RET phosphorylation assays

Phosphorylation of RET was assessed as previously described (Leppanen, Bespalov et al. 2004). MG87 RET cells were plated on 35 mm tissue culture dishes, left to attach to the surface overnight and then transfected with 4 µg/dish of GFRα1-expressing plasmid using Lipofectamine 2000 (Invitrogen) for DNA delivery as described by manufacturer. Next day cells were starved for 4 hr in serum-free DMEM containing 15 mM HEPES, pH 7.2 and 1% DMSO and stimulated with 5-100 µM compounds or GDNF (200 ng/ml) for 15 min diluted in serum-free DMEM containing 15 mM HEPES, pH 7.2 and 1% DMSO. Afterwards, cells were washed once with ice-cold PBS containing 1 mM Na₃VO₄ and lysed on ice in 0.5 ml per well of RIPA-modified buffer (50 mM Tris-HCl, pH 7.4, 150 mM NaCl, 1 mM EDTA, 1% NP-40, 1% triton-X100, 10% glycerol, EDTA-free EASYpack, protease inhibitor cocktail (Roche), 1 mM Na₃VO₄, 2.5 mg/ml of sodium deoxycholate). Plates were incubated on horizontal shakers for 30 min with vigorous shaking, lysates were collected in Eppendorf tubes and centrifuged in a microfuge for 10 min at 6000g at 4°C to precipitate cell debris. Supernatants were incubated overnight with 2 µg/ml of anti-RET C-20 antibodies (Santa-Cruz Biotechnology, Inc., sc-1290) and protein G-conjugated beads (Thermo Fisher Scientific, Cat # 10004D). Beads were washed 3 times with 1x TBS (50 mM Tris-HCl, pH 7.4, 150 mM NaCl) with 1% triton X-100, bound proteins were eluted by 50 µl of 2x Laemmli loading buffer, resolved on 7.5% SDS-PAGE and then transferred to a nitrocellulose membrane. Total phosphorylated residues were then probed using the 4G10 antibody (1:1,000, Millipore, Cat # 05-321) followed by anti-mouse antibodies conjugated with horse radish peroxidase (1 : 1,500, DAKO, Cat# P0447) in TBS-T containing 3% skimmed milk. To confirm equal loading, membranes were stripped, washed, blocked, and re-probed with anti-RET C-20 antibodies (1:500, Santa-Cruz Biotechnology, Inc.) followed by anti-goat antibodies conjugated with horse radish peroxidase (1:1,500, DAKO, Cat# P0449) in TBS-T containing 3% skimmed milk. Stained bands were visualized with ECL or femptoECL reagent (Pierce) using LAS-3000 imaging system (Fuji).

Surface Plasmon Resonance (SPR)

Binding interactions between the small molecules (4 mM stocks of compounds 8 and 9 in 5% (v/v) DMSO) and human RET protein (R&D Systems #1168-CR/CF) were

examined at 25°C using a BIACORE T200 system (GE Healthcare Bio-Sciences AB, Uppsala, Sweden; Control software v2.0 and Evaluation software v1.0). Protein-grade Tween 20 and Empigen detergents (Anatrace #APT020 and #D350, respectively), anhydrous DMSO (Sigma #276855), Pierce Gentle Ag/Ab Elution buffer (Thermo Fisher #21027) and all other chemicals were reagent grade quality. The carrier-free proteins were immobilized to S-series CM5 sensors (10 µg/ml RET in 10 mM sodium acetate pH 5.5) using the Biacore Amine Coupling Kit as recommended by the manufacturer (1500 – 5000 RU final density) in PBS-T running buffer (10 mM phosphate, pH 7.4; 150 mM NaCl; 0.05% (v/v) Tween-20). Corresponding reference surfaces were prepared in the absence of protein. The immobilized surfaces were active as confirmed by binding of specific anti-Ret monoclonal antibodies (0.25 mg/ml stock, Abcam ab134100) in dose-dependent binding. Between titration series, the surfaces were regenerated at 50 µl/min using two 30 sec pulses of solutions I (0.1% (v/v) Empigen in Pierce Gentle Elution buffer), II (1.0 M NaCl and 0.1% (v/v) Empigen in 50 mM HCl), and III (1.0 M NaCl and 0.1% (v/v) Empigen in 50 mM NaOH).

Using PBS-T containing 5% (v/v) DMSO, fixed 100 µM concentrations of compound 9 (negative) and compound 8 (positive) were injected in-tandem over reference and protein-immobilized surfaces at 25 µl/min (60 sec association, 60-180 sec dissociation) to establish binding specificity. To examine binding kinetics and affinity, compound 8 was titrated in single-cycle (25 µl/min x 1 sec association + 60-600 sec dissociation) and multi-cycle (10 µl/min x 10 min association + 20 min dissociation) mode. Between titration series, the surfaces were regenerated at 50 µl/min using two 30 sec pulses of solutions I (1.0 M NaCl and 0.1% (v/v) Empigen in PBST-DMSO), II (1.0 M NaCl and 0.1% (v/v) Empigen in 50 mM NaOH), and III (50 mM NaOH).

Biochemical Assays

For biochemical assays, cells were seeded onto 6-well plates (0.4 x 10⁶ cells/well) and cultured overnight. Cells were serum-starved for 2 hr and then stimulated with compounds for 20 minutes before preparation of cell lysates in 100 µl lysis buffer (20 mM Tris-HCl pH 7.5, 137 mM NaCl, 2 mM EDTA, 1% Nonidet P-40) containing a protease inhibitor cocktail. Lysates were centrifuged at 4°C for 10 minutes at 6000g,

prior to protein quantification using the Bradford assay (BioRad). After SDS-PAGE, Western transfer to PVDF membranes, and blocking steps, an overnight incubation at 4°C with the primary antibodies pAkt, pErk, total Akt, total Erk (Cell Signaling, catalogue #4060, #4370, #9272, #9102), Actin (Sigma Aldrich, catalogue A2066), RETpY¹⁰⁶² (a gift from Dr. Brian Pierchala) were used at a 1:2,000 dilution, with secondary 1:10,000. Signals were developed using Western Lightning Plus ECL (PerkinElmer), films were scanned and quantified using ImageJ software. Controls for protein loading for each sample were standardized to total Akt, total Erk or Actin.

Primary Cultures

E18 primary cortical neurons from mouse were purchased frozen (BrainBits LLC). For biochemical assays, 0.25×10^6 cells were plated in 12-well plates coated with poly-D-lysine, and cultured for 5 days in commercial neurobasal media (NbActiv1). Half of the media was exchanged every 2 days. Following the culture period, the media was removed and replaced with serum-free DMEM for a 3-hour starvation. Treatments were 20 minutes, and lysates were prepared as described above.

Cell Survival Assays

Cell survival was measured by the MTT assay using optical density readings as the endpoint. 2000-5000 cells were plated in 96-well format in serum-free media (SFM) (HCell-100, Wisent) and vehicle or test agents at concentrations of 5 μ M and 10 μ M were added. The positive control growth factors (GF) were used at optimal concentrations (30 ng/ml GDNF for MG87 RET/GFR α 1, 25 ng/ml FGF2 for MG87 RET, 30 ng/ml NGF for MG87 TrkA). FGF2 was used for MG87 RET cells as they do not respond to GDNF in the absence of GFR α 1. Assay time was typically 72 hr, at which point MTT reagent (Sigma Aldrich) was added. Assays were repeated at least 3 times. MTT optical density (OD) data were standardized to growth factor = 100%, and SFM = 0%, using the formula $[(OD_{\text{test}} - OD_{\text{SFM}}) * 100 / (OD_{\text{GF}} - OD_{\text{SFM}})]$.

Compounds

Test compounds were acquired from the NCI/DTP repository (<http://dtp.cancer.gov>), through searches of the PubChem Compound database (Kim, Thiessen et al. 2016). Upon receipt, structures were coded for simplicity. The original identifiers and IUPAC names are: 4-amino-8-hydroxynaphthalene-2,6-disulfonic acid (NSC37051) **compound 7 (CAS 6271-90-5)**; 5-amino-4-hydroxynaphthalene-1,6-disulfonic acid (NSC37052) **compound 8 (CAS 6271-89-2)**; (3Z)-6-amino-4-oxo-3-(phenylhydrazinylidene)naphthalene-2,7-disulfonic acid (NSC45189) **compound 9 (CAS 6222-38-4)**; 5-amino-3-[[4-[4-[(4-amino-2-methylphenyl)diazenyl]phenyl]sulfanylphenyl]hydrazinylidene]-6-[(4-nitrophenyl)diazenyl]-4-oxonaphthalene-2,7-disulfonic acid (NSC65571) **compound 15 (CAS 6950-40-9)**; 4-amino-3-[(2,5-dichlorophenyl)diazenyl]-5-oxo-6-[[4-[4-[2-(4-oxocyclohexa-2,5-dien-1-ylidene)hydrazinyl]phenyl]sulfanylphenyl]hydrazinylidene]naphthalene-2,7-disulfonic acid (NSC75661) **compound 23**; (3E)-5-amino-3-[[4-[4-[(4-amino-6-sulfonaphthalen-1-yl)diazenyl]phenyl]phenyl]hydrazinylidene]-6-[(4-nitrophenyl)diazenyl]-4-oxonaphthalene-2,7-disulfonic acid (NSC77520) **compound 24**; 4-amino-3-[(4-nitrophenyl)diazenyl]-5-oxo-6-[[4-[4-[2-(4-oxocyclohexa-2,5-dien-1-ylidene)hydrazinyl]phenyl]sulfanylphenyl]hydrazinylidene]naphthalene-2,7-disulfonic acid (NSC79723) **compound 28**; (3Z)-5-amino-3-[[4-[4-[(2,4-diamino-5-methylphenyl)diazenyl]phenyl]phenyl]hydrazinylidene]-6-[(2,5-dichlorophenyl)diazenyl]-4-oxonaphthalene-2,7-disulfonic acid (NSC79730) **compound 29**; 4-amino-3-[[4-[4-[(1-amino-5-sulfonaphthalen-2-yl)diazenyl]phenyl]phenyl]diazenyl]-5-oxo-6-(phenylhydrazinylidene)naphthalene-2,7-disulfonic acid (NSC79745) **compound 35 (CAS 6486-54-0)**; (3Z)-5-amino-3-[[4-[4-[(2,4-diamino-3-methyl-6-sulfophenyl)diazenyl]phenyl]phenyl]hydrazinylidene]-6-[(3-nitrophenyl)diazenyl]-4-oxonaphthalene-2,7-disulfonic acid (NSC80903) **compound 36**.

SU5416 was purchased from Tocris (Cat. # 3037), and XIB4035 was purchased from Sigma (Cat. # SML1159).

Synthesis and structural characterization of compounds

See **Supplemental** information. **Compound 8** was misannotated in the NCI library, and the correct structure is reported here. Other compounds were annotated correctly.

Animal models

All animal procedures respected the IACUC guidelines for use of animals in research, and to protocols approved by McGill University Animal Welfare Committees. All animals were housed 12 hr dark-light cycle with food and water *ad libitum*. We used the “RHOP347S” transgenic mouse (expressing the human Rhodopsin mutated at amino acid position 347) in a C57BL/6J (B6) background (kindly donated by Dr. T. Li) (Li, Snyder et al. 1996). This model of RP faithfully replicates the features of disease progression in humans. Both male and female animals were used in the experiments. For retinal cultures, animals at post-natal day 18 weighing between 10-12 g were used. For intravitreal injections and histochemical studies, animals 8 weeks of age were used, weighing between 20-25 g.

Retinal Organotypic Cultures

Whole eyes were enucleated and whole retinas dissected from wild-type and RHOP347S mice at post-natal day 18 were used for organotypic culture experiments. Following enucleation, eyes were placed in a petri dish with PBS. The cornea was perforated and cut away along the ora serrata, leaving room to remove the lens. Whole intact retinas were then freely dissected away from the sclera and immediately transferred into 24 well plates containing 500 μ l of culture medium (DMEM/F12 supplemented with 10 mM NaHCO₃, 100 μ g/ml Transferrin, 100 μ M Putrescine, 20 nM Progesterone, 30 nM Na₂SeO₃, 0.05 mg/ml Gentamicin, 2 mM L-Glutamine, and 1 mM Sodium Pyruvate). Under sterile conditions, the media was gently removed and replaced with fresh media containing the treatments or controls, and incubated at 37°C and 5% CO₂ for 24 hr. Compounds were tested at a concentration of 20 μ M, GDNF at 500 ng/ml. Cell grade DMSO was used for vehicle treatments and was 0.5% by volume. Retinas were then used for TUNEL staining.

TUNEL staining

Staining was performed using the DeadEnd Fluorometric TUNEL system (Promega). RHOP347S retinas in culture (n=4 for GDNF treatments, n=3 for test compounds)

were first fixed in 4% PFA in PBS and kept at 4°C overnight. Three quick washes in PBS-0.2% BSA were done the next day, followed by three 30-minute permeabilization steps using 2% Triton X-100 in PBS. Retinas were then incubated with 20 µg/mL Proteinase K in PBS for 15 minutes, briefly re-fixed in 4% PFA in PBS for 30 minutes and washed again with PBS-0.2% BSA before being transferred into Eppendorf tubes. Samples were incubated with 50 µl of equilibration buffer for 20 minutes, then 25 µl of TdT reaction mixture for 2.5 hr at 37°C. The reaction was terminated using a 30 minute incubation of 2X SSC solution. The retinas were mounted with the ganglion-cell layer facing up using Vectashield with DAPI. For image acquisition, the retinas were divided into 4 quadrants, and 3 pictures with a 20X objective were taken in each area (central, mid, peripheral) for a total of 12 images of the outer-nuclear layer (ONL) per retina. Total TUNEL-positive cells were counted in each image semi-automatically (ImageJ). Counts were verified by at least one other person blinded to the experimental conditions. Wild-type retinal flat mounts were used as negative controls.

Immunohistochemistry

After enucleation, the eyes were immersed overnight in fixative composed of 4% PFA in PBS at 4°C, followed by cryoprotection by soaking in 30% sucrose overnight at 4°C. Eyes were frozen in O.C.T tissue TEK and cryostat sections were cut and mounted onto gelatin-coated glass slides. Sections (14 µm thick) were washed with PBS and then incubated in PBS containing 3% normal goat serum, 0.2% Triton X-100 and 3% bovine serum albumin (BSA) for 2 hr. After, sections were incubated overnight at 4°C with primary antibody (1:250 p-MAPK, Cell Signaling #4370; 1:250 p-Akt, Cell Signaling #4060; 1:400 CRALBP, Abcam ab183728). The sections were rinsed and incubated with secondary antibody for 1 hr at room temperature. Then, sections were washed and coverslipped using Vectashield mounting media with DAPI.

Image acquisition (fluorescence microscopy) and data analysis

Pictures were taken as Z-stacks of confocal optical sections using a Leica confocal microscope at a 20X objective. Images were equally adjusted using Adobe Photoshop CS 8.0 to remove background signals.

For each experimental condition, a minimum of 6 images were acquired from 3 sections cut from different areas of the retina (n=3 retinas per group). The area of the profiles of the cells expressing pErk and pAkt was measured using ImageJ software.

Intravitreal injections

Mice were anesthetized with isoflurane, delivered through a gas anesthetic mask. The treatments were delivered using a Hamilton syringe. Injections were done using a surgical microscope to visualize the Hamilton entry into the vitreous chamber and confirm delivery of the injected solution. 3 μ l of a 2 mM stock solution composed of 50% DMSO in PBS were delivered. After the injection, the syringe was left in place for 30 seconds and slowly withdrawn from the eye to prevent reflux. Experimental right eyes were injected with the test agents and left eyes served as the vehicle-injected internal control.

Statistical analyses

The quantitative data were subjected to statistical analyses using GraphPad Prism 5 software, and are presented as mean \pm SD for all studies. The differences between groups were determined by ANOVA (multiple groups) followed by Dunnett's or Bonferroni-corrected t-tests. Student t-tests were performed to compare two groups. p-values below 0.05 were considered to indicate statistically significant differences between groups. The number of experimental replicates was pre-determined based on the level of variation observed in previous work, and each experiment was reproduced the number of times indicated. The nature of the experiments are exploratory, and as such are not testing a pre-specified null hypothesis. P-values are therefore meant to be descriptive in their interpretation.

Results

In vitro screening: Identification of selective RET agonists

Initial hits emerged and were identified by a luciferase-reporter assay (Sidorova, Matlik et al. 2010) monitoring Erk activation in cells expressing GDNF receptors. Selected compounds (NCI/DTP chemical repository, and the PubChem database) (Kim, Thiessen et al. 2016) were screened at 5 and 20 μ M concentrations (**Supplemental Table 1**). A small family of compounds that increased luciferase activity >1.5 times, consistently in more than three independent luciferase-reporter assays, were considered candidates for further study.

Candidates, coded 15, 23, 24, 28, 29, 35, and 36, were tested in biochemical assays for stimulation of RET phosphorylation (pRET), and downstream phosphorylation of Akt (pAkt) and Erk (pErk) using transfected MG87 fibroblasts stably expressing either RET only or RET/GFR α 1 (untransfected or TrkA-transfected MG87 cells were used as controls). Structures are shown in **Supplemental Figure 1**. Cells were treated with compounds, DMSO vehicle (negative control), or GDNF (positive control), and lysates were analyzed by Western blot for pRET (specific antibody to RET-pY¹⁰⁶²), pAkt and pErk.

Compounds 15, 24, 28, 29, 35, and 36 were active and generated pAkt and pErk signals in MG87 RET/GFR α 1 cells. The RET-pY¹⁰⁶² does not yield a quantifiable signal (**Figure 1A**), but pAkt and pErk quantifications are shown (**Figure 1B**). Biochemical activation by compounds was comparable to the optimal dose of GDNF. Compound 23 was not active, though it is a structural analog of the active compounds.

In MG87 RET cells compounds 15, 24, 28, 29, 35, and 36 also activate RET in the absence of GFR α 1 (**Figure 1C**, quantified in **Figure 1D**); but, as GDNF requires the presence of GFR α 1 receptor, GDNF was not active in these cells. Note that the compounds activate RET in the absence of GFR α 1, but GFR α 1 expression dampens RET activation by some compounds (especially at the lower concentrations of 5-10 μ M). An example of dose-dependent activation of RET, Akt and Erk is shown for compound 29 (**Figure 1E**).

To evaluate RET selectivity and RET dependence, counter-screens were performed using the MG87 TrkA cell line expressing the TrkA receptor tyrosine kinase. In MG87

TrkA cells the positive control is Nerve Growth Factor (NGF), and vehicle and compound 23 were used as negative controls. Compound 35, an agonist of RET, did not activate any signals in MG87 TrkA cells. There were no increases in pErk, pAkt or pTrkA compared to negative control compound 23 or to vehicle (**Figure 1F**). In positive controls, NGF increased pTrkA, pAkt and pErk levels. Hence, compound 35 appears to be RET-selective or dependent on RET-expression. Compound 35 was selected for further studies.

Optimization of selective RET agonists

Analogs of compound 35 in the NCI database yield compounds 7, 8, and 9, also procured from the NCI (structures are listed in **Supplemental Figure 1**). In MG87 RET/GFR α 1 cells, compound 8 acted as a RET agonist and significantly increased pAkt and pErk, (**Figure 2A**, quantified in **2B**). Compound 7 also appeared to exhibit some activity, with a biased trend for pErk. Compound 9 was inactive.

In MG87 RET cells (lacking GFR α 1) compound 8 activated RET and significantly increased the levels of RET downstream targets pAkt and pErk, and all other compounds and GDNF were inactive (**Figure 2C**, quantified in **2D**). While remaining non-significant, the same biased pErk signaling profile for compound 7 was observed in these cells as well.

RET selectivity was tested in counter-screens using MG87 TrkA cells. Compounds 7, 8, and 9 did not generate pAkt or pErk or pTrkA signals, while positive control Nerve Growth Factor (NGF) activated these signals (**Figure 2E**, quantified in **2F**). These data indicate that compound 8 (like parental compound 35) remains RET-selective or RET-dependent, and does not require co-expression of GFR α 1, while compounds 7 and 9 are negative controls.

Signaling was further evaluated in E18 mouse primary cortical neurons which endogenously express RET and GFR α 1, and respond to GDNF (Catapano, Arnold et al. 2001, Bonafina, Fontanet et al. 2018). Increases in pAkt were detectable following treatment with GDNF (200 ng/ml) or compound 8 (10 and 20 μ M) (**Figure 2G**). These data confirm RET activation by compound 8 in primary neurons.

Agonism by compound 8 requires the RET kinase to be active. In MG87 RET/GFR α 1 cells, the pAkt and pErk induced by GDNF or by compound 8 are completely ablated when cells are pre-treated with RET kinase inhibitor SU5416 (Mologni, Sala et al. 2006) (**Figure 2H**).

Compound 8 is a RET ligand

We examined the kinetics and affinity of RET-compound 8 interactions using real-time surface plasmon resonance (SPR). Recombinant human RET extracellular ectodomain was amine-coupled to SPR sensors, with reference sensor having no protein. A fixed concentration (100 μ M) screening of compound 8 to RET-coated surfaces showed substantial binding with slow dissociation kinetics (**Figure 3A**). Under the same binding conditions and on the same chip, inactive compound 9 failed to interact with RET (**Figure 3A**).

Dose-dependent titrations (**Figure 3B**) showed that on low-density RET surfaces compound 8 generated signals (e.g. 150 RU at 12.5 μ M and 230 RU at 25 μ M, see arrows). Complementary multi-cycle analyses indicated that compound 8 has sub-micromolar affinity for RET (**Figure 3C**). After the binding studies using titrations of the compound, we verified that immobilized RET protein was still present on chip surfaces as it was bound by anti-RET monoclonal antibodies (mAb). The anti-RET mAb generated signals correlating binding to the low-density and the high-density RET-loaded chip surfaces (**Figure 3D**). These data indicate that compound 8 is a genuine ligand of the RET ectodomain.

Compound 8 induces signals through RET phosphorylation

Taken together, the data strongly support RET as the main target for the panel of molecules tested. Moreover compound 8 binds to RET directly.

Compound 8 and compound 9 (negative control) were selected for dose-dependent studies in MG87 RET/GFR α 1 cells. From lysates prepared from treated or control cells, RET was immunoprecipitated, and total pTyr was quantified by western blotting.

This technique allows the direct detection and quantification of pRET. The data show dose-dependent induction of pRET by compound 8, comparable to GDNF, while

compound 9 was inactive over the full concentration range (**Figure 3E**, quantified in **3G**). Similar experiments in MG87 RET cells showed that compound 8 induces detectable increases in pRET whether or not cells express GFR α 1 (**Figure 3F**).

These data demonstrate that RET is a pharmacological target for compound 8, and corroborate the biochemical findings that GFR α 1 is not necessary for the compound to induce signaling. However, we note that the 50-100 μ M concentrations that induce significant pRET levels are higher than the 5-20 μ M concentrations that afford detection of pAkt and pErk. This can be explained by signal amplification, and by the transient nature of pRET which reportedly is difficult to detect because it is rapidly targeted for degradation (Pierchala, Milbrandt et al. 2006). Therefore, small, undetectable changes in phospho-RET may lead to much larger increases in the effectors pAkt and pErk.

Small molecule RET activation does not require GFR α 1 expression but is regulated by GFR α 1 likely via an allosteric mechanism

Given that compound 8 induces RET-pY¹⁰⁶², a phosphotyrosine linked to the survival promoting effect of GDNF in neurons (Runeberg-Roos and Saarma 2007, Ibanez 2013) we quantified in MTT assays the cell survival / active metabolism as a biological correlate of the biochemical data.

MG87 RET, MG87 RET/GFR α 1, and MG87 TrkA cells were treated with test compounds 7 and 8. Inactive compound 9 and vehicle were used as negative controls. As positive controls we used growth factors: FGF2 for MG87 RET (as these cells lacking GFR α 1 do not respond to GDNF), GDNF for MG87 RET/GFR α 1, and NGF for MG87 TrkA. The growth factors as positive controls were used at their optimal concentrations to afford maximal cell viability, which was set to 100%. Cells were cultured for 72 hr under serum-free conditions \pm treatments.

In MG87 RET cells compounds 7 and 8 (5-10 μ M) supported viability to a significant ~25% of control FGF2 (**Figure 4A**), and GDNF was inactive because these cells lack GFR α 1. In MG87 RET/GFR α 1 cells compounds 7 and 8 (5-10 μ M) supported viability to ~10% (non-significant) compared to control GDNF (**Figure 4B**). Control compound 9 was inactive in all cell lines, as anticipated.

In MG87 RET/GFR α 1 cells, at 10 μ M compound 8 does not afford significant cell survival (**Figure 4B**), but signal transduction is significant (**Figure 2**). The discrepancy between biological (cell survival) and biochemical (pTyr) signals may be due to expression of GFR α 1 negatively regulating ligand binding or long-term survival. A similar phenomenon was reported for GDNF mutants (Eketjall, Fainzilber et al. 1999). Hence, higher concentrations of compound 8 were evaluated in biological assays.

In MG87 RET/GFR α 1 cells compound 8 at 40 μ M supported viability to a significant ~65% of GDNF levels, while compound 9 remained inactive (**Figure 4B**). In counter-assays using MG87 TrkA cells compounds 7 and 8 (as well as compound 9) were inactive at all concentrations, compared to positive control NGF (N) (**Figure 4C**).

Overall, these biological data demonstrate that compound 8 binds RET, and acts as a selective RET agonist that –unlike GDNF– does not require GFR α 1 co-receptors. Compound 8 via RET phosphorylation activates signal transduction pathways that afford neuronal survival independent of GFR α 1 co-receptors. However, expression of GFR α 1 co-receptors appear to modulate the long-term survival-promoting action of compound 8. The GFR α 1 repression can be overcome with higher concentrations of compound 8, which achieve better cell survival.

Pharmacological modulation of the regulation by GFR α 1

To interrogate how GFR α 1 regulates compound 8-mediated activation of RET, we used XIB4035, an agent reported to modulate GFR α 1 without having intrinsic signaling activity (Hedstrom, Murtie et al. 2014).

In MG87 RET/GFR α 1 cells, pre-treatment with 4 μ M XIB4035 for 20 minutes completely blocked the biochemical signals activated by compound 8, without inhibiting GDNF signals. Cellular controls using MG87 TrkA cells showed that XIB4035 had no effect on either NGF or FGF2 growth factor signaling, demonstrating that the XIB4035 block is selective (**Figure 4D**).

Hence, expression of unbound GFR α 1 negatively modulates the RET signals that are activated by compound 8, and this modulation can be overcome with higher concentrations of compound 8. Moreover, the GFR α 1 bound by XIB4035 inhibits compound 8 activation of RET even more strongly. Given that compound 8 is a genuine

ligand of RET (see SPR studies, **Fig. 3**) we infer that the repression of compound 8 activation of RET by unbound GFR α 1 (and the even stronger inhibition by bound GFR α 1•XIB4035) likely occurs through an allosteric mechanism.

This concept would be useful for devising screening strategies. While the GFR α 1 ligand XIB4035 exacerbates RET inhibition, it is conceivable that there may be GFR α 1 ligands that reduce RET inhibition, and potentially could even allow ligand-independent activation of RET.

Compound 8 reduces photoreceptor apoptosis in a retinitis pigmentosa model, and activates pErk and pAkt *in vivo*

Compound 8 was tested for neuroprotective capabilities in the mutant RHOP347S transgenic mouse model of retinitis pigmentosa. This mutation of the *rhodopsin* gene causes a highly aggressive phenotype with ~50% photoreceptor death by post-natal day 18, and nearly complete loss by post-natal day 28 (Li, Snyder et al. 1996).

Organotypic cultures of RHOP347S retinas from post-natal day 18 mice cultured for 24 hr exhibit TUNEL-positive staining in the photoreceptor layer (indicating apoptosis), with other retinal structures remaining free of apoptosis (**Figure 5A**). Controls using retinal explants from wild-type mice resulted in very low or absent TUNEL signal.

Compound 8 (20 μ M) affords a significant ~25% decrease in TUNEL-positive cells indicating neuroprotection in RHOP347S retinas. Representative pictures from the central retina (the region surrounding the optic nerve) demonstrate the reduction in TUNEL-positive cells (**Figure 5A**). In contrast, GDNF (500 ng/ml) did not reduce TUNEL counts compared to vehicle. These data indicate that compound 8 possesses disease-modifying capabilities in the degenerating retina, with an efficacy that is above GDNF under the conditions evaluated. These data highlight the potential utility of using small, selective ligands over large proteins like GDNF as therapeutics.

To further evaluate compound 8 *in vivo*, it was delivered by intravitreal injection in wild-type mice. In each mouse, one eye served as the test eye, and the contralateral eye received control vehicle. Retinal sections were prepared 1 hr later, and pErk and pAkt levels were analyzed by immunohistochemistry.

The effectors pAkt (**Figure 5B**) and pErk (**Figure 5C**) were increased after treatment with compound 8, mainly in Müller cells as confirmed by co-localization with the glial marker cellular retinaldehyde binding-protein (CRALBP). This is consistent with Müller cells expressing RET (Hauck, Kinkl et al. 2006, Del Rio, Irmeler et al. 2011). High pErk and pAkt were noted particularly in the Müller glial cell processes and fibers projecting towards the photoreceptors. The retinal pErk and pAkt increases were a significant ~3-fold and ~2-fold respectively compared to vehicle (quantified in **Figure 5D**). We were unable to localize pRET in these retinas, as the anti-pRET antibody does not label tissues, and activated pRET is rapidly targeted for degradation (Pierchala, Milbrandt et al. 2006).

These data indicate that compound 8 is bioactive *in vivo* in the mouse retina, and the neuroprotective effect seen in the experiments above likely derives from Müller glia supporting the photoreceptor population in a paracrine manner.

Compound 8 is incorrectly curated in the NCI library

In an effort to develop structure-activity relationships, and to generate new chemical entities, we attempted synthesis of analogs of compound 8. Surprisingly, the in-house synthesized compound 8 and its derivatives were inactive.

Thus, we analyzed in detail the identity of compound 8 procured from the NCI, though the amount of material provided was quite limiting. Reverse-phase HPLC analysis revealed that NCI compound 8 has a major peak with 90% of the material, and the remaining material was a mixture (**Supplemental Figure 2**). The major fraction was isolated and characterized.

The mass of compound 8 (ESI Mass Spec) that we obtained matched that reported by the NCI, however the ¹H-NMR spectra revealed an inconsistency with the proposed structure (**Supplemental Figure 3**). The triplet observed around 7.4ppm suggested an aromatic proton with two neighboring protons. This resonance is not possible given the side-group configuration of compound 8 reported in the NCI database. However, this resonance pattern and the mass are consistent with a positional isomer 4-Amino-5-hydroxy-1,3-naphthalenedisulfonic acid.

We acquired 4-Amino-5-hydroxy-1,3-naphthalenedisulfonic acid commercially (TCI), and this isomer had a mass and ¹H-NMR spectra matching that of compound 8. The two agents (NCI-compound 8 and 4-Amino-5-hydroxy-1,3-naphthalenedisulfonic acid) also co-eluted in Reverse-phase HPLC under different buffer conditions, confirming a likely incorrect structural assignment of compound 8 at the NCI database.

Following these findings, we also examined mass spectra of other compounds 15, 23, 29, and 35. The mass of all these agents are reported correctly in the NCI database. Moreover, ¹H-NMR spectra of compounds 29 and 35 are consistent with the structures reported in the NCI database, and they are likely correct. While the binding and the bioactivity we report for compound 8 (and other compounds) are conclusive, these findings serve as a cautionary note when screening large chemical databases. Further structural elucidation and synthesis of the bioactive component of compound 8 is under investigation.

Discussion

We have characterized a novel class of small molecules that can activate RET. The small molecules provide improved RET receptor specificity compared to GDNF which requires GFR α 1 for activating RET (Sariola and Saarma 2003, Gash, Zhang et al. 2005, Touchard, Heiduschka et al. 2012), and binds to other targets such as heparan sulphate proteoglycans (Bespalov et al. 2011).

RET-selective ligands were useful as a chemical biology tool to evaluate GFR α 1•RET functional interactions. We show that expression of GFR α 1 (in the unliganded state) dampens the trophic efficacy of compound 8, while in the bound state (with XIB4035) it further inhibits pAkt/pErk signals induced by compound 8. The data highlights the dynamic relationships that exist between RET and GFR α 1 receptors.

RET-selective ligands were useful also as neuroprotective agents, and compared to GDNF, are superior therapeutics *ex vivo* and *in vivo*, reducing neuronal death.

RET-dependent signals and selectivity, possible mechanism of action, and the influence of GFR α 1

Compound 8 is a genuine ligand of RET ectodomain. Compound 8 and related small drug-like compounds activate the intracellular downstream effectors Akt and Erk. Distinct from GDNF, the compounds activate RET in cells lacking the GFR α 1 co-receptor. The agents do not affect GDNF functionally, do not require GDNF or GFR α 1 to produce biological effects, and appear to be RET-selective.

There are other reported small molecule “GDNF mimetics” acting as RET agonists, (Saarma, Karelson et al. 2011, Bespalov, Sidorova et al. 2016, Sidorova, Bespalov et al. 2017, Ivanova, Tammiku-Taul et al. 2018). For example, BT13 is a selective RET agonist, however it suffers from low solubility and has poor pharmacological properties, as also do other reported agents. Moreover, BT13 and other agents reportedly compete with GDNF binding; hence if used as therapeutics they would reduce any benefit provided by endogenous GDNF. Another agent XIB4035 acts as a GFR α 1 modulator, but it requires the presence of GDNF and acts only on cells co-expressing RET/GFR α 1 (Tokugawa, Yamamoto et al. 2003, Hedstrom, Murtie et al. 2014).

We speculate that the RET-activating agents we report here may be allosteric, though this notion remains unproven. Analysis of the RET/GFR α 1 interface revealed a potential allosteric binding site for small molecules (Ivanova, Tammiku-Taul et al. 2018). An allosteric mechanism would be consistent with the ligand-independent regulation of GFR α 1 upon RET (Treanor, Goodman et al. 1996), and observations that mutant forms of GDNF with low affinity for GFR α 1 binding can signal through RET but require GFR α 1 to be present (Eketjall, Fainzilber et al. 1999).

RET is a receptor tyrosine kinase (RTK), a family of receptors generally considered to require homodimerization and/or a conformational reorganization of homodimers for activation. It is unlikely that the small molecules would be capable of inducing RET dimerization given their small size and limited surfaces, and the fact that they are asymmetrical and most likely monovalent. However, all RTKs exist at equilibrium between monomeric and dimeric (or oligomeric) forms in the absence ligand, such that a small molecule could induce a conformational change within a preformed receptor complex. This 'dynamic equilibrium' phenomenon has been shown for other neurotrophin RTKs (Maliartchouk, Debeir et al. 2000, Maliartchouk, Feng et al. 2000, Mischel, Umbach et al. 2002), and was suggested for RET (Bespalov and Saarma 2007).

Compound 8 rescues MG87 RET cells from serum-deprivation induced death, but to rescue MG87 RET/GFR α 1 cells it required relatively high concentrations, well beyond those needed for pAkt and pErk activation. While the small molecules activate signals in the absence of GFR α 1, agonism leading to cell survival can be partially suppressed by the presence of GFR α 1. The partial suppression of RET activation by GFR α 1 can be overcome by increasing the concentration of compound 8, further suggesting an allosteric impact or an influence on ligand affinity. This is consistent with discrepancies between biochemical signals and biological outcomes reported for GDNF (Lindgren, Leak et al. 2008). GDNF-activated RET signaling can be progressively dampened by increasing expression levels of GFR α 1 (Trupp, Raynoschek et al. 1998).

Since GFR α 1 also determines the cellular localization of activated RET to lipid rafts, which in turn can influence signaling, perhaps this is a mechanism for GFR α 1 suppression of RET activation by compound 8. The functional antagonism of compound

8 (a RET-activator) by XIB4035 (a reported GFR α 1 ligand) further suggests a ligand-dependent allosteric cross-regulation.

Comparable to the functional cross-talk between GFR α 1–RET described here, there are reported agonists of Trk receptors (Maliartchouk, Feng et al. 2000, Zaccaro, Lee et al. 2005, Massa, Yang et al. 2010) whose function can be regulated by p75^{NTR} co-receptors. Regulation can be allosteric, with the ligands promoting Trk-p75 interactions, or with the ligands unmasking a cryptic receptor hot spot (Zaccaro, Ivanisevic et al. 2001, Ivanisevic, Banerjee et al. 2003, Guillemard, Ivanisevic et al. 2010).

Therapeutic utility

GDNF plays an important neuroprotective role in the developing and the adult retina, supporting neuronal populations. Transgenic mice expressing human rhodopsin with a proline-serine substitution at residue 347 faithfully replicate the RP disease, and were chosen for our studies (Li, Snyder et al. 1996). Compound 8-induced RET signaling translated into a functional neuroprotective effect, with a significantly reduced number of TUNEL counts in the ONL, compared to vehicle. In contrast, GDNF itself failed to reduce TUNEL counts with concentrations up to 500 ng/ml (using recombinant GDNF produced in *E. coli*, or in mammalian CHO cells).

The reason for the failure of GDNF in our therapeutic experiments is possibly due to the fact that we used a single dose, attempting to evaluate a translational paradigm. Other studies, including those of degeneration due to RP either employ multiple doses or achieve sustained GDNF expression and release (McGee Sanftner, Abel et al. 2001, Gregory-Evans, Chang et al. 2009, Ohnaka, Miki et al. 2012). GDNF can also fail due to clearance after binding to extracellular matrix and transmembrane heparin sulphate proteoglycans and other proteins upregulated in the degenerating retina (Landers, Rayborn et al. 1994).

RP is one of the most common forms of inherited visual loss, affecting over a million people worldwide, and is the result of about 400 possible mutations in any one of multiple genes such as rhodopsin. The RP disease is characterized by progressive degeneration of photoreceptors initiated by the mutant rhodopsin, followed by retinal pigmented epithelium stress, and toxic/oxidative/pro-inflammatory damage to the visual

system and irreversible blindness (Guadagni, Novelli et al. 2015). There is no cure or effective treatment. Given that RP is the result of one of many possible mutations in any one of multiple genes, the availability of a small molecule neuroprotective agent would allow treatment of a broad spectrum of patients regardless of disease etiology.

Intravitreal administration of compound 8 induced pErk and pAkt in Müller cells, consistent with other reports using GDNF and related growth factors (Wahlin, Campochiaro et al. 2000, Hauck, Kinkl et al. 2006). Our results support the notion of a non-cell autologous mechanism where neuroprotective signals likely originate from Müller glia acting in a paracrine fashion. This concept is consistent with the fact that ectopic expression of RET on photoreceptors failed to protect them from degeneration (Allocca, Di Vicino et al. 2007), and papers suggesting an indirect rescue of photoreceptors either through mitigation of toxic events within the retina, or by inducing paracrine release of trophic factors which then act on target neurons (Hauck, Kinkl et al. 2006, Koeberle and Bahr 2008, Del Rio, Irmeler et al. 2011).

Chemical Database Screening: A cautionary tale

Chemical libraries are a valuable resource for research initiatives. However, there continue to be complications. This is especially relevant given the rise of high-throughput screening techniques, when often the data reported are not sufficient for others to interpret and/or replicate (Inglese, Shamu et al. 2007). While some chemical repositories do explicitly state that they cannot assure the contents of their libraries, they are also not permitted to provide adequate details in the case of a discrepancy. This is the case for compound 8 and its derivatives where supplier information and storage conditions cannot be provided by the NCI (personal correspondence).

The situation here is similar to the discovery of TIC10/ONC20, an anti-cancer therapeutic agent. TIC10/ONC201 emerged from a screen from the NCI library, and the structure had been only partially documented using mass spectroscopy (Allen, Krigsfeld et al. 2013). Inconsistencies led to the finding that the real active molecule was in fact an isomer of the structure reported by the NCI (Jacob, Lockner et al. 2014), and both the mixture as well as the correct compound were used for clinical development. In both TIC10/ONC201 and compound 8 the lack of a precise structure does not undermine the

biological data reported. However, considerable efforts must be directed at identifying the active component of compound 8 for future studies and reproducibility.

Overall, our work demonstrates the concept that it is possible to develop small molecule RET agonists that do not require GFR α 1, and which are devoid of many of the therapeutic hurdles of the GDNF protein. Using small molecules as probes, regulation of agonist-induced RET signals by GFR α 1 is demonstrated. The data highlight the utility and advantages small molecules offer with respect to target validation and receptor biology.

Acknowledgements

We are thankful for reagents provided by Dr. Brian Pierchala (pRET antibodies), Dr. Eero Castren (MG87/Trk cell lines), Dr. Carlos Ibanez (MG87/RET cell lines), and Dr. T. Li (RHOP347S transgenic mice). Jenni Montonen assisted with the Ret phosphorylation assays. Dr. Enrique de la Rosa (Spain) assisted with retinal explants and TUNEL assays.

Disclosures

Patent applications have been filed on behalf of authors (HUS, SJ, MS, and YS).

Authorship Contributions

Participated in research design: Jmaeff, H.U Saragovi

Conducted experiments: Jmaeff, Sidorova, Lippiatt, Barcelona, Nedev, Hancock

Contributed new reagents or analytic tools: Nedev

Performed data analysis: Jmaeff, Sidorova, Lippiatt, Hancock, Saarma, L. Saragovi

Wrote or contributed to the writing of the manuscript: Jmaeff, Sidorova, Hancock, Saarma, H.U. Saragovi

References

- Airaksinen, M. S. and M. Saarma (2002). "The GDNF family: signalling, biological functions and therapeutic value." *Nat Rev Neurosci* **3**(5): 383-394.
- Allen, J. E., G. Krigsfeld, P. A. Mayes, L. Patel, D. T. Dicker, A. S. Patel, N. G. Dolloff, E. Messaris, K. A. Scata, W. Wang, J. Y. Zhou, G. S. Wu and W. S. El-Deiry (2013). "Dual inactivation of Akt and ERK by TIC10 signals Foxo3a nuclear translocation, TRAIL gene induction, and potent antitumor effects." *Sci Transl Med* **5**(171): 171ra117.
- Allocca, M., U. Di Vicino, M. Petrillo, F. Carlomagno, L. Domenici and A. Auricchio (2007). "Constitutive and AP20187-induced Ret activation in photoreceptors does not protect from light-induced damage." *Invest Ophthalmol Vis Sci* **48**(11): 5199-5206.
- Bespalov, M. M. and M. Saarma (2007). "GDNF family receptor complexes are emerging drug targets." *Trends Pharmacol Sci* **28**(2): 68-74.
- Bespalov, M. M., Y. A. Sidorova, I. Suleymanova, J. Thompson, O. Kambur, V. Jokinen, T. Lilius, G. Karelson, L. Puusepp, P. Rauhala, E. Kalso, M. Karelson and M. Saarma (2016). "Novel agonist of GDNF family ligand receptor RET for the treatment of experimental neuropathy." [bioRxiv](https://doi.org/10.1101/061111).
- Bonafina, A., P. A. Fontanet, G. Paratcha and F. Ledda (2018). "GDNF/GFRalpha1 Complex Abrogates Self-Renewing Activity of Cortical Neural Precursors Inducing Their Differentiation." *Stem Cell Reports* **10**(3): 1000-1015.
- Boucher, T. J., K. Okuse, D. L. Bennett, J. B. Munson, J. N. Wood and S. B. McMahon (2000). "Potent analgesic effects of GDNF in neuropathic pain states." *Science* **290**(5489): 124-127.
- Brantley, M. A., Jr., S. Jain, E. E. Barr, E. M. Johnson, Jr. and J. Milbrandt (2008). "Neurturin-mediated ret activation is required for retinal function." *J Neurosci* **28**(16): 4123-4135.
- Catapano, L. A., M. W. Arnold, F. A. Perez and J. D. Macklis (2001). "Specific neurotrophic factors support the survival of cortical projection neurons at distinct stages of development." *J Neurosci* **21**(22): 8863-8872.
- Del Rio, P., M. Irmeler, B. Arango-Gonzalez, J. Favor, C. Bobe, U. Bartsch, E. Vecino, J. Beckers, S. M. Hauck and M. Ueffing (2011). "GDNF-induced osteopontin from Muller glial cells promotes photoreceptor survival in the Pde6brd1 mouse model of retinal degeneration." *Glia* **59**(5): 821-832.
- Eketjall, S., M. Fainzilber, J. Murray-Rust and C. F. Ibanez (1999). "Distinct structural elements in GDNF mediate binding to GFRalpha1 and activation of the GFRalpha1-c-Ret receptor complex." *EMBO J* **18**(21): 5901-5910.
- Gash, D. M., Z. Zhang, Y. Ai, R. Grondin, R. Coffey and G. A. Gerhardt (2005). "Trophic factor distribution predicts functional recovery in parkinsonian monkeys." *Ann Neurol* **58**(2): 224-233.
- Gregory-Evans, K., F. Chang, M. D. Hodges and C. Y. Gregory-Evans (2009). "Ex vivo gene therapy using intravitreal injection of GDNF-secreting mouse embryonic stem cells in a rat model of retinal degeneration." *Mol Vis* **15**: 962-973.
- Guadagni, V., E. Novelli, I. Piano, C. Gargini and E. Strettoi (2015). "Pharmacological approaches to retinitis pigmentosa: A laboratory perspective." *Prog Retin Eye Res* **48**: 62-81.
- Guillemand, V., L. Ivanisevic, A. G. Garcia, V. Scholten, O. M. Lazo, F. C. Bronfman and H. U. Saragovi (2010). "An agonistic mAb directed to the TrkC receptor juxtamembrane region defines a trophic hot spot and interactions with p75 coreceptors." *Dev Neurobiol* **70**(3): 150-164.
- Hamilton, J. F., P. F. Morrison, M. Y. Chen, J. Harvey-White, R. S. Pernaute, H. Phillips, E. Oldfield and K. S. Bankiewicz (2001). "Heparin coinfusion during convection-enhanced delivery (CED) increases the distribution of the glial-derived neurotrophic factor (GDNF) ligand family in rat striatum and enhances the pharmacological activity of neurturin." *Exp Neurol* **168**(1): 155-161.

- Hauck, S. M., N. Kinkl, C. A. Deeg, M. Swiatek-de Lange, S. Schoffmann and M. Ueffing (2006). "GDNF family ligands trigger indirect neuroprotective signaling in retinal glial cells." *Mol Cell Biol* **26**(7): 2746-2757.
- Hedstrom, K. L., J. C. Murtie, K. Albers, N. A. Calcutt and G. Corfas (2014). "Treating small fiber neuropathy by topical application of a small molecule modulator of ligand-induced GFRalpha/RET receptor signaling." *Proc Natl Acad Sci U S A* **111**(6): 2325-2330.
- Hubin, T. J., J. M. McCormick, S. R. Collinson, M. Buchalova, C. M. Perkins, N. W. Alcock, P. K. Kahol, A. Rahghunathan and D. H. Busch (2000). "New Iron(II) and Manganese (II) Complexes of Two Ultra-Rigid, Cross Bridges Tetraazamacrocyclic for Catalysis and Biomimicry." *J. Am. Chem. Soc.* **122**: 2512-2522.
- Ibanez, C. F. (2013). "Structure and physiology of the RET receptor tyrosine kinase." *Cold Spring Harb Perspect Biol* **5**(2).
- Inglese, J., C. E. Shamu and R. K. Guy (2007). "Reporting data from high-throughput screening of small-molecule libraries." *Nat Chem Biol* **3**(8): 438-441.
- Ivanisevic, L., K. Banerjee and H. U. Saragovi (2003). "Differential cross-regulation of TrkA and TrkC tyrosine kinase receptors with p75." *Oncogene* **22**(36): 5677-5685.
- Ivanova, L., J. Tammiku-Taul, A. T. Garcia-Sosa, Y. Sidorova, M. Saarma and M. Karelson (2018). "Molecular Dynamics Simulations of the Interactions between Glial Cell Line-Derived Neurotrophic Factor Family Receptor GFRalpha1 and Small-Molecule Ligands." *ACS Omega* **3**(9): 11407-11414.
- Ivanova, L., J. Tammiku-Taul, Y. Sidorova, M. Saarma and M. Karelson (2018). "Small-Molecule Ligands as Potential GDNF Family Receptor Agonists." *ACS Omega* **3**(1): 1022-1030.
- Jacob, N. T., J. W. Lockner, V. V. Kravchenko and K. D. Janda (2014). "Pharmacophore reassignment for induction of the immunosurveillance cytokine TRAIL." *Angew Chem Int Ed Engl* **53**(26): 6628-6631.
- Joseph-Hernandez, S., S. Jmaeff, I. Pirvulescu, T. Aboukassim and H. U. Saragovi (2017). "Neurotrophin receptor agonists and antagonists as therapeutic agents: An evolving paradigm." *Neurobiol Dis* **97**(Pt B): 139-155.
- Kim, S., P. A. Thiessen, E. E. Bolton, J. Chen, G. Fu, A. Gindulyte, L. Han, J. He, S. He, B. A. Shoemaker, J. Wang, B. Yu, J. Zhang and S. H. Bryant (2016). "PubChem Substance and Compound databases." *Nucleic Acids Res* **44**(D1): D1202-1213.
- Koeberle, P. D. and M. Bahr (2008). "The upregulation of GLAST-1 is an indirect antiapoptotic mechanism of GDNF and neurturin in the adult CNS." *Cell Death Differ* **15**(3): 471-483.
- Landers, R. A., M. E. Rayborn, K. M. Myers and J. G. Hollyfield (1994). "Increased retinal synthesis of heparan sulfate proteoglycan and HNK-1 glycoproteins following photoreceptor degeneration." *J Neurochem* **63**(2): 737-750.
- Leppanen, V. M., M. M. Bessalov, P. Runeberg-Roos, U. Puurand, A. Merits, M. Saarma and A. Goldman (2004). "The structure of GFRalpha1 domain 3 reveals new insights into GDNF binding and RET activation." *EMBO J* **23**(7): 1452-1462.
- Li, T., W. K. Snyder, J. E. Olsson and T. P. Dryja (1996). "Transgenic mice carrying the dominant rhodopsin mutation P347S: evidence for defective vectorial transport of rhodopsin to the outer segments." *Proc Natl Acad Sci U S A* **93**(24): 14176-14181.
- Lindgren, N., R. K. Leak, K. M. Carlson, A. D. Smith and M. J. Zigmond (2008). "Activation of the extracellular signal-regulated kinases 1 and 2 by glial cell line-derived neurotrophic factor and its relation to neuroprotection in a mouse model of Parkinson's disease." *J Neurosci Res* **86**(9): 2039-2049.
- Maliartchouk, S., T. Debeir, N. Beglova, A. C. Cuello, K. Gehring and H. U. Saragovi (2000). "Genuine monovalent ligands of TrkA nerve growth factor receptors reveal a novel pharmacological mechanism of action." *J Biol Chem* **275**(14): 9946-9956.
- Maliartchouk, S., Y. Feng, L. Ivanisevic, T. Debeir, A. C. Cuello, K. Burgess and H. U. Saragovi (2000). "A designed peptidomimetic agonistic ligand of TrkA nerve growth factor receptors." *Mol Pharmacol* **57**(2): 385-391.

- Massa, S. M., T. Yang, Y. Xie, J. Shi, M. Bilgen, J. N. Joyce, D. Nehama, J. Rajadas and F. M. Longo (2010). "Small molecule BDNF mimetics activate TrkB signaling and prevent neuronal degeneration in rodents." *The Journal of Clinical Investigation* **120**(5): 1774-1785.
- McGee Sanftner, L. H., H. Abel, W. W. Hauswirth and J. G. Flannery (2001). "Glial cell line derived neurotrophic factor delays photoreceptor degeneration in a transgenic rat model of retinitis pigmentosa." *Mol Ther* **4**(6): 622-629.
- Mischel, P. S., J. A. Umbach, S. Eskandari, S. G. Smith, C. B. Gundersen and G. A. Zampighi (2002). "Nerve growth factor signals via preexisting TrkA receptor oligomers." *Biophys J* **83**(2): 968-976.
- Mologni, L., E. Sala, S. Cazzaniga, R. Rostagno, T. Kuoni, M. Puttini, J. Bain, L. Cleris, S. Redaelli, B. Riva, F. Formelli, L. Scapozza and C. Gambacorti-Passerini (2006). "Inhibition of RET tyrosine kinase by SU5416." *J Mol Endocrinol* **37**(2): 199-212.
- Nutt, J. G., K. J. Burchiel, C. L. Comella, J. Jankovic, A. E. Lang, E. R. Laws, Jr., A. M. Lozano, R. D. Penn, R. K. Simpson, Jr., M. Stacy, G. F. Wooten and I. G. S. G. I. i. G. c. l.-d. n. factor (2003). "Randomized, double-blind trial of glial cell line-derived neurotrophic factor (GDNF) in PD." *Neurology* **60**(1): 69-73.
- Ohnaka, M., K. Miki, Y. Y. Gong, R. Stevens, T. Iwase, S. F. Hackett and P. A. Campochiaro (2012). "Long-term expression of glial cell line-derived neurotrophic factor slows, but does not stop retinal degeneration in a model of retinitis pigmentosa." *J Neurochem* **122**(5): 1047-1053.
- Pierchala, B. A., J. Milbrandt and E. M. Johnson, Jr. (2006). "Glial cell line-derived neurotrophic factor-dependent recruitment of Ret into lipid rafts enhances signaling by partitioning Ret from proteasome-dependent degradation." *J Neurosci* **26**(10): 2777-2787.
- Runeberg-Roos, P. and M. Saarma (2007). "Neurotrophic factor receptor RET: structure, cell biology, and inherited diseases." *Ann Med* **39**(8): 572-580.
- Saarma, M., M. Karelson, M. Beshpalov and M. Pilv (2011). Methods of facilitating neural cell survival using gdnf family ligand (gfl) mimetics or ret signaling pathway activators, Google Patents.
- Salvatore, M. F., Y. Ai, B. Fischer, A. M. Zhang, R. C. Grondin, Z. Zhang, G. A. Gerhardt and D. M. Gash (2006). "Point source concentration of GDNF may explain failure of phase II clinical trial." *Exp Neurol* **202**(2): 497-505.
- Sariola, H. and M. Saarma (2003). "Novel functions and signalling pathways for GDNF." *J Cell Sci* **116**(Pt 19): 3855-3862.
- Sidorova, Y. A., M. M. Beshpalov, A. W. Wong, O. Kambur, V. Jokinen, T. O. Lilius, I. Suleymanova, G. Karelson, P. V. Rauhala, M. Karelson, P. B. Osborne, J. R. Keast, E. A. Kalso and M. Saarma (2017). "A Novel Small Molecule GDNF Receptor RET Agonist, BT13, Promotes Neurite Growth from Sensory Neurons in Vitro and Attenuates Experimental Neuropathy in the Rat." *Front Pharmacol* **8**: 365.
- Sidorova, Y. A., K. Matlik, M. Paveliev, M. Lindahl, E. Piranen, J. Milbrandt, U. Arumae, M. Saarma and M. M. Beshpalov (2010). "Persephin signaling through GFRalpha1: the potential for the treatment of Parkinson's disease." *Mol Cell Neurosci* **44**(3): 223-232.
- Tokugawa, K., K. Yamamoto, M. Nishiguchi, T. Sekine, M. Sakai, T. Ueki, S. Chaki and S. Okuyama (2003). "XIB4035, a novel nonpeptidyl small molecule agonist for GFRalpha-1." *Neurochem Int* **42**(1): 81-86.
- Touchard, E., P. Heiduschka, M. Berdugo, L. Kowalczyk, P. Bigey, S. Chahory, C. Gandolphe, J. C. Jeanny and F. Behar-Cohen (2012). "Non-viral gene therapy for GDNF production in RCS rat: the crucial role of the plasmid dose." *Gene Ther* **19**(9): 886-898.
- Treanor, J. J., L. Goodman, F. de Sauvage, D. M. Stone, K. T. Poulsen, C. D. Beck, C. Gray, M. P. Armanini, R. A. Pollock, F. Hefti, H. S. Phillips, A. Goddard, M. W. Moore, A. Buj-Bello, A. M. Davies, N. Asai, M. Takahashi, R. Vandlen, C. E. Henderson and A. Rosenthal (1996). "Characterization of a multicomponent receptor for GDNF." *Nature* **382**(6586): 80-83.
- Trupp, M., C. Raynoschek, N. Belluardo and C. F. Ibanez (1998). "Multiple GPI-anchored receptors control GDNF-dependent and independent activation of the c-Ret receptor tyrosine kinase." *Mol Cell Neurosci* **11**(1-2): 47-63.

Wahlin, K. J., P. A. Campochiaro, D. J. Zack and R. Adler (2000). "Neurotrophic factors cause activation of intracellular signaling pathways in Muller cells and other cells of the inner retina, but not photoreceptors." *Invest Ophthalmol Vis Sci* **41**(3): 927-936.

Whone, A., M. Luz, M. Boca, M. Woolley, L. Mooney, S. Dharia, J. Broadfoot, D. Cronin, C. Schroers, N. U. Barua, L. Longpre, C. L. Barclay, C. Boiko, G. A. Johnson, H. C. Fibiger, R. Harrison, O. Lewis, G. Pritchard, M. Howell, C. Irving, D. Johnson, S. Kinch, C. Marshall, A. D. Lawrence, S. Blinder, V. Sossi, A. J. Stoessl, P. Skinner, E. Mohr and S. S. Gill (2019). "Randomized trial of intermittent intraputamenal glial cell line-derived neurotrophic factor in Parkinson's disease." *Brain* **142**(3): 512-525.

Zaccaro, M. C., L. Ivanisevic, P. Perez, S. O. Meakin and H. U. Saragovi (2001). "p75 Co-receptors regulate ligand-dependent and ligand-independent Trk receptor activation, in part by altering Trk docking subdomains." *J Biol Chem* **276**(33): 31023-31029.

Zaccaro, M. C., H. B. Lee, M. Pattarawarapan, Z. Xia, A. Caron, P. J. L'Heureux, Y. Bengio, K. Burgess and H. U. Saragovi (2005). "Selective small molecule peptidomimetic ligands of TrkC and TrkA receptors afford discrete or complete neurotrophic activities." *Chem Biol* **12**(9): 1015-1028.

MOL # 118950

Footnote

This work was supported by the Sean Murphy Award given to SJ, grants from the Canadian Institutes of Health Research (Pharmacology) and from the US Department of Defense (Optic Nerve Trauma W81XWH1910853) to HUS, a grant from the Finnish Academy (N1325555) to YS, and the Lundbeck Foundation and the Sigrid Jusélius Foundation to MS. The McGill SPR-MS Facility was supported by the Canada Foundation for Innovation (CFI grant #228340) for the BIACORE T200 SPR infrastructure.

Figure Legends

Figure 1. Characterization of RET agonists.

(A-B) Biochemical studies of RET activators in MG87 RET/GFRa1 cells. Following serum deprivation, cells were treated with DMSO vehicle (V), 10 ng/ml GDNF (G), or 20 μ M compounds for 20 min. Representative blot shown, cell lysates were probed for pRET-Y¹⁰⁶², pAkt, and pErk. Total Akt and Erk used as loading controls. Increases in pRET-Y¹⁰⁶² were seen, however compounds generated large increases particularly in pAkt and pErk, with the exception of compound 23. **(C-D)** Biochemical studies of RET activators in MG87 RET cells, lacking GFRa1. Representative blot shown, demonstrating relevant signaling by this panel of compounds. Note that GDNF is inactive in this cell type, and compound 23 remains inactive. **(E)** Western blots showing dose-dependent RET activation by compound 29 (2.5-20 μ M) in both MG87 RET/GFRa1 and MG87 RET cells, further suggesting GFRa1 independence. **(F)** Counter screens for selectivity in MG87 TrkA cells. Western blot quantification of NGF (N) at 30 ng/ml (positive control), or the selected compound 35 at 20 μ M. Compound 23 was used as a negative control. Compound 35 demonstrated the most favorable selectivity as it did not activate Akt or Erk in MG87 TrkA cells lacking RET. Western blot data were quantified from 3 independent experiments, expressed as mean \pm SD and standardized to Vehicle control. For pAkt * $p < 0.05$, ** $p < 0.005$, *** $p < 0.0005$. For pErk, # $p < 0.05$, ## $p < 0.005$, ### $p < 0.0005$, Dunnett's test.

Figure 2. Lead optimization.

(A-B) Biochemical studies with compound 35 derivatives in MG87 RET/GFRa1 cells assayed 20 μ M concentrations of compounds 7, 8, and 9 with a 20 min exposure time. Representative Western blot shown for RET-pY¹⁰⁶² and its effectors pAkt and pErk. GDNF (G) is GDNF positive control and vehicle (V) is the DMSO negative control. Compound 8 displayed a signaling profile which mirrored that of the parent compounds, while compound 7 generated a pErk biased signaling trend. Compound 9 was completely inactive. **(C-D)** Biochemical studies with compound 35 derivatives tested in MG87 RET cells. Representative Western blot shown for RET-pY¹⁰⁶² and its effectors pAkt and pErk. GDNF (G) is GDNF positive control and vehicle (V) is the DMSO negative control. Signaling profiles of compounds 7,8, and 9 were similar to those observed in MG87 GFRa1/RET cells, indicative these derivatives maintained GFRa1 independence. **(E-F)** Selectivity screens in MG87 TrkA cells, using 20 μ M concentrations of compound 35 derivatives, stimulated for 20 min. Representative blot for pTrkA and its effectors pAkt and pErk. NGF (N) is positive control and vehicle (V) is the negative control. Compounds 7,8, and 9 were all inactive in these assays. **(G)** Compound 8 signaling in E18 mouse cortical neurons. Neurons were treated with compound 9 at 20 μ M, GDNF at 100 and 200 ng/ml, and compound 8 at 10 μ M and 20 μ M, for 20 min. Representative blot showing pAkt increases observed with both treatments of compound 8. Actin was used as loading control. **(H)** RET inhibition blocks compound 8 signaling. MG87 RET/GFRa1 cells were first treated with the RET antagonist SU5416 at 10 μ M for 20 min, and then additionally for 20 min with GDNF (G) or compound 8. Vehicle (V) and SU5416 (S) alone are controls. SU5416 pre-treatment resulted in clear reductions in the signaling capacity of both GDNF and compound 8. Representative blot showing pAkt and pErk, with Actin as loading control. Vehicle (V) is the negative control. In panels **B**, **D**, and **F**, quantification of western blot data was standardized to total Erk or total Akt and expressed as mean \pm SD from 3 independent experiments. For pAkt * p <0.05, ** p <0.005, *** p <0.0005. For pErk # p <0.05, ## p <0.005, ### p <0.0005 versus Vehicle, Dunnett's test.

Figure 3. Compound 8 is a RET ligand that induces RET tyrosine phosphorylation

(A) Surface Plasmon Resonance, real-time binding to recombinant human RET ectodomain. Representative, reference-subtracted SPR for sequential injections of buffer (PBS-T containing 2% (v/v) DMSO), compound 9 (100 μ M, negative control), and compound 8 (100 μ M) over amine-coupled high-density RET (4600 RU, *solid black line*) at 25 μ L/min (60 sec association). **(B)** Representative single-cycle SPR data for compound 8 (0 – 25 μ M; 2-fold dilution series) injected over amine-coupled low-density RET (1650 RU, *solid black line*) at 25 μ L/min (60 sec association +/- 60-600 sec dissociation). Arrows indicate injection times. **(C)** Representative multi-cycle SPR data for compound 8 (0 – 20 μ M; 2-fold dilution series) injected over 1650 RU RET surface at 25 μ L/min (600 sec association + 900 sec dissociation); experimental titration series (*grey lines*) were fit globally to “1:1 kinetic” model in BIAevaluation software (*black lines*). **(D)** Representative single-cycle SPR data for anti-RET monoclonal antibody (0 – 210 nM; 2-fold dilution series) injected over 4600 RU RET (*solid black line*), and 1650 RU RET (*dashed black line*) surfaces at 25 μ L/min (60 sec association +/- 60-600 sec dissociation). **(E-G)** Compound 8 induces RET phosphorylation in a dose-dependent manner. MG87 RET/GFRa1 or MG87 RET cells were treated for 15 min with compound 8, or control compound 9, at a concentration range of 5-100 μ M, or controls GDNF (G) at 200 ng/ml, or vehicle (V). RET protein was immunoprecipitated and probed with 4G10 mAb (detecting phosphotyrosine). Compound 9 was inactive at all concentrations, whereas compound 8 induced a marked increase in phosphorylated RET whether or not cells express GFRa1. In MG87 RET/GFRa1 cells compound 8 at 50 μ M was as effective GDNF at 200 ng/ml. Quantification in panel G was standardized to total RET protein and expressed as mean \pm SD from 3 independent experiments. ** $p < 0.005$, *** $p < 0.0005$ versus Vehicle, Dunnett’s test.

Figure 4. RET-mediated trophic signals activated by compound 8 are regulated by GFRa1.

(A) Compound 35 derivatives mediate survival in MG87 RET cells. Cells under serum starvation for 72 hr were treated with DMSO Vehicle (V), FGF (as these cells are insensitive to GDNF), or compounds 7, 8, and 9; at 5 and 10 μ M concentrations. Cell survival/metabolism was assessed via the MTT assay. 10 μ M concentrations of compound 7 or compound 8 yielded appreciable survival levels; whereas compound 9 was inactive, as expected. (B) Compound 35 derivatives do not afford survival in MG87 RET/GFRa1 cells under the same conditions. In these cells, GDNF yielded significant survival while the trophic effects of compounds 7 and 8 diminished, suggesting a negative influence of the GFRa1 receptor. MG87 RET/GFRa1 survival increased with higher concentrations of compound 8, and reached significance at 40 μ M, suggesting a negative regulatory role of GFRa1 expression on the functional outcome. (C) Compound 35 derivatives demonstrate selectivity as measured by cell survival. MTT assays conducted in the MG87 TrkA cell line, covering the full concentration range of 5 to 40 μ M for each compound, were standardized to positive control NGF (N) and compared against Vehicle (V). All compounds were completely inactive in this cell type, including GDNF (G). (D) Biochemical studies on the influence of GFRa1 and compound 8. MG87 RET/GFRa1 or MG87 TrkA cells were pretreated with 4 μ M XIB4035 (a GFRa1 modulator) for 10 minutes before the addition of compound 8 at 10 μ M, GDNF (G), NGF (N), or FGF2 (F). XIB4035 blocked the signaling of compound 8, but did not affect GDNF. Control experiments in the TrkA expressing cells showed that XIB4035 did not impact either NGF or FGF2 signals, overall supporting the negative regulatory role of GFRa1 specifically on compound 8 signaling. MTT Data are expressed as % survival relative to optimal growth factor \pm SD from 6 independent experiments (each experiment n=4-8 replicate wells which were averaged). For each cell type, the respective trophic factor was standardized to 100%, and vehicle to 0%. * p <0.05, *** p<0.0005, Dunnett's test versus inactive compound 9.

Figure 5. Compound 8 is neuroprotective in the RHOP347S model of RP and activates Akt and Erk in retinal Müller Glial cells.

(A) Compound 8 reduces neuronal death. Whole retinas of post-natal day 18 RHOP347S mice were dissected for organotypic culture. Each paired set of retinas (left and right of the same mouse) were treated with either compound 8 at 20 μ M or GDNF at 500 ng/ml in one retina, and DMSO vehicle (V) as control in the other retina. In a separate series of experiments, an inactive compound was also tested as control at 20 μ M. Cultures were kept for 24 hr, then TUNEL staining was performed. Representative TUNEL images taken at 20x in the central retina are shown. Scale bar = 25 μ m. Quantification of TUNEL-positive photoreceptors in the ONL shows that treatment with 8 reduces apoptosis, while GDNF had no effect. Data expressed as TUNEL-positive cells per $\text{mm}^2 \pm \text{SD}$, ** $p < 0.005$, Bonferroni-corrected t-test. (B-D) Compound 8 activates signals *in vivo*. Young adult mice (8 weeks old) were injected intravitreally (2 μ g) with compound 8 in one eye or DMSO Vehicle in the contralateral eye. Eyecups were collected after 1 hr and sectioned. Compound 8 increased pAkt in the inner nuclear layer, as well as in fibers projecting from cell bodies in the inner nuclear layer (Müller cell bodies). These signals co-localized with the Müller cell marker CRALBP. Compound 8 also increased pErk in the inner nuclear layer, as well as in fibers projecting from cell bodies in the inner nuclear layer (Müller cell bodies) towards the ONL where the cell body of photoreceptors reside. These signals co-localized with the Müller cell marker CRALBP. Scale bar = 25 μ m. RGC = retinal ganglion cell layer, INL= Inner nuclear layer, ONL = outer nuclear layer. Quantification of pAkt and pErk (n=3 per group) expressed as the fold-change in pixel area over vehicle $\pm \text{SD}$, *** $p < 0.0005$, Student t-test, ** $p < 0.005$, Student t-test.

Figure 1

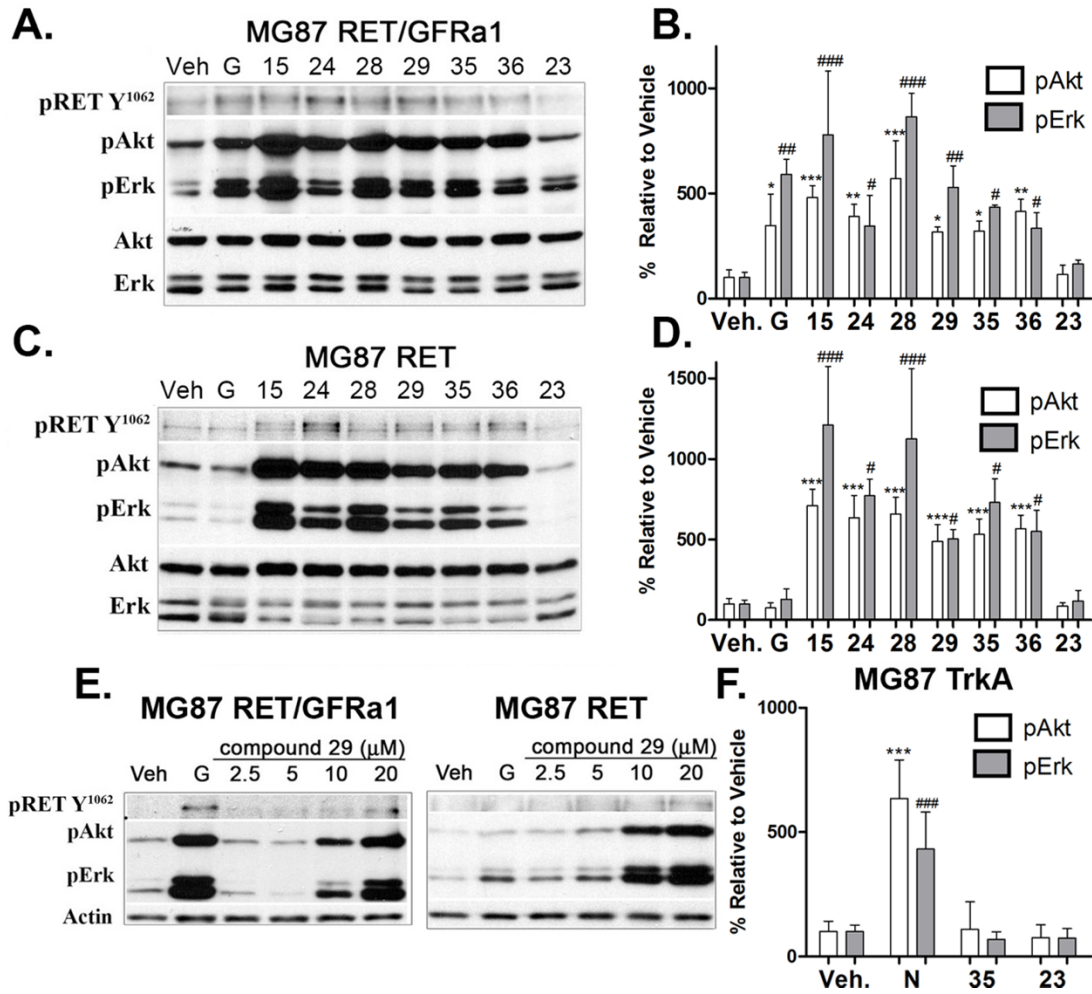


Figure 2

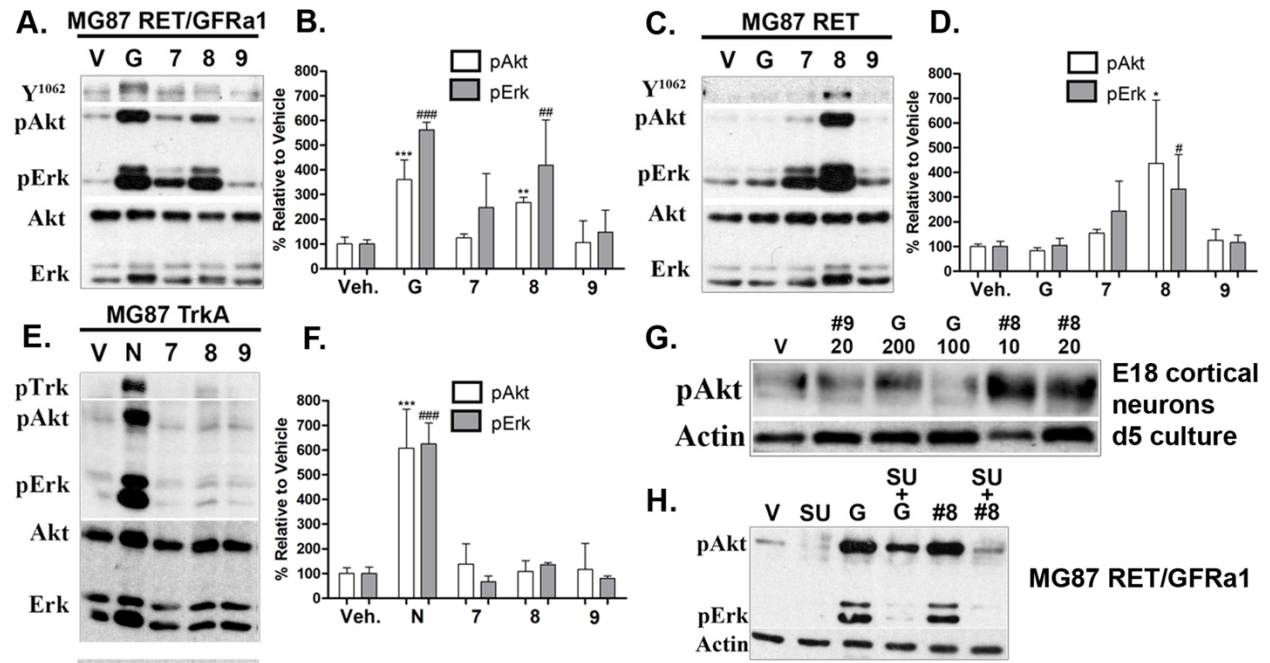


Figure 3

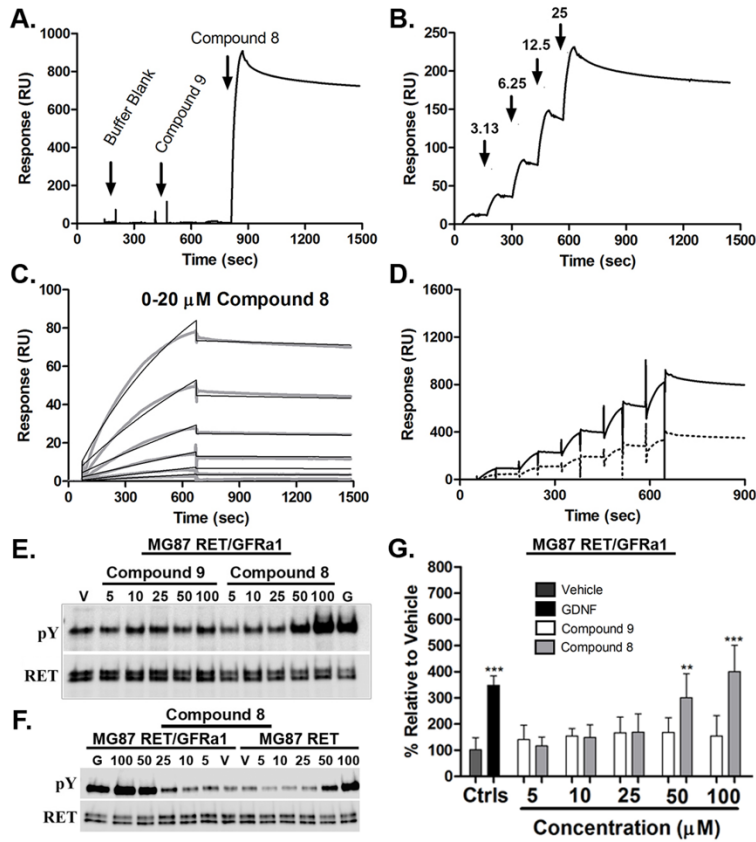


Figure 4

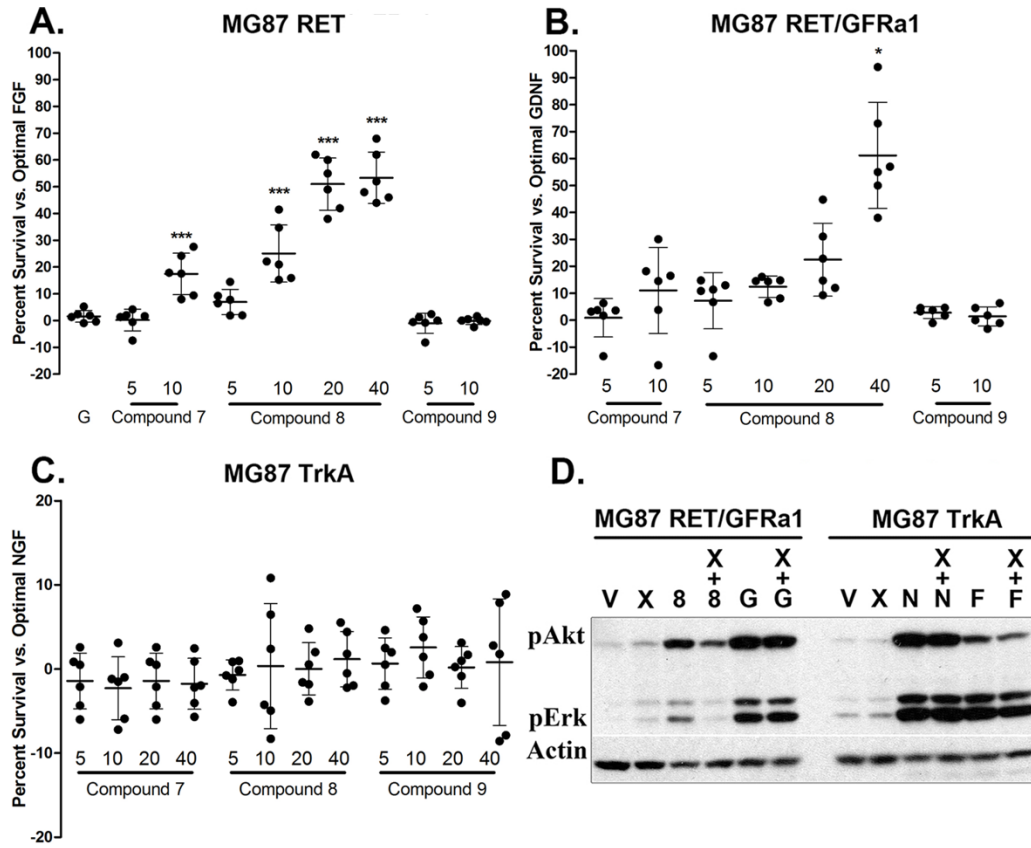
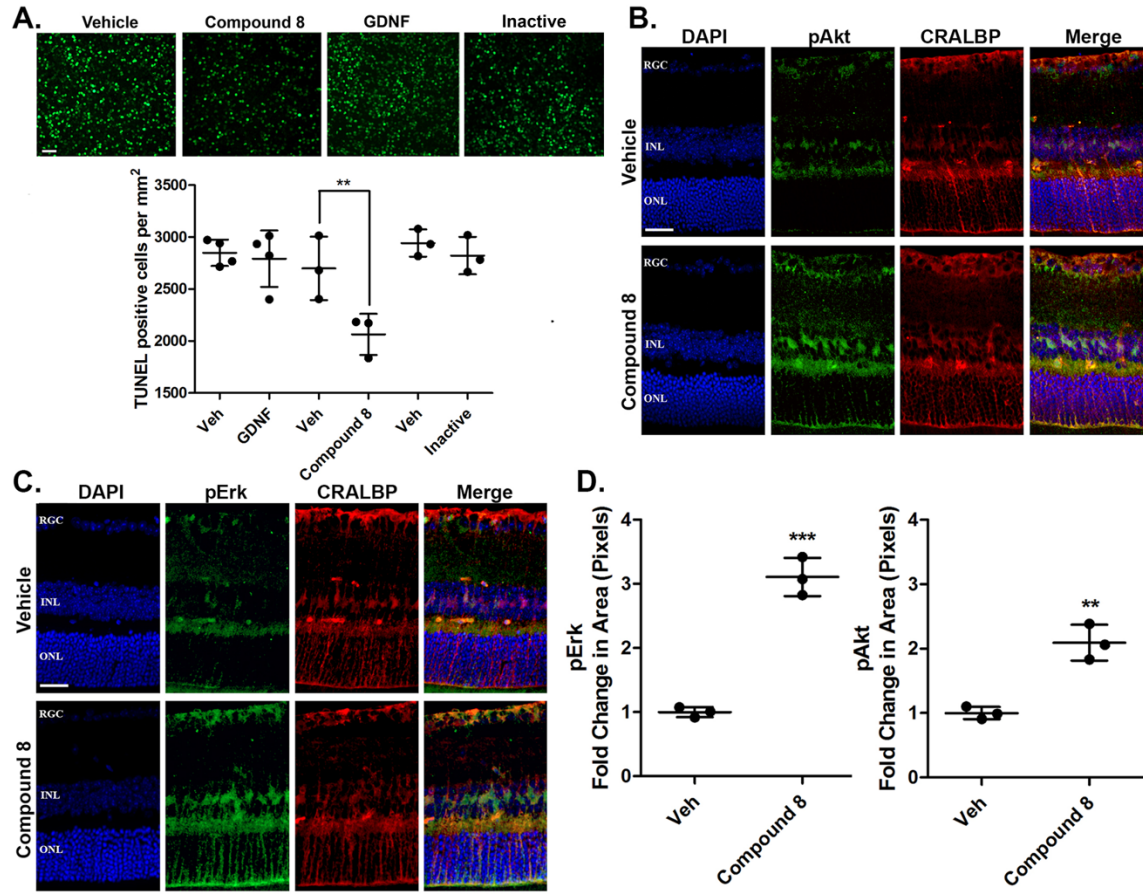


Figure 5



Supplemental Data

Small-molecule ligands that bind the RET receptor activate neuroprotective signals independent of but modulated by co-receptor GFR α 1

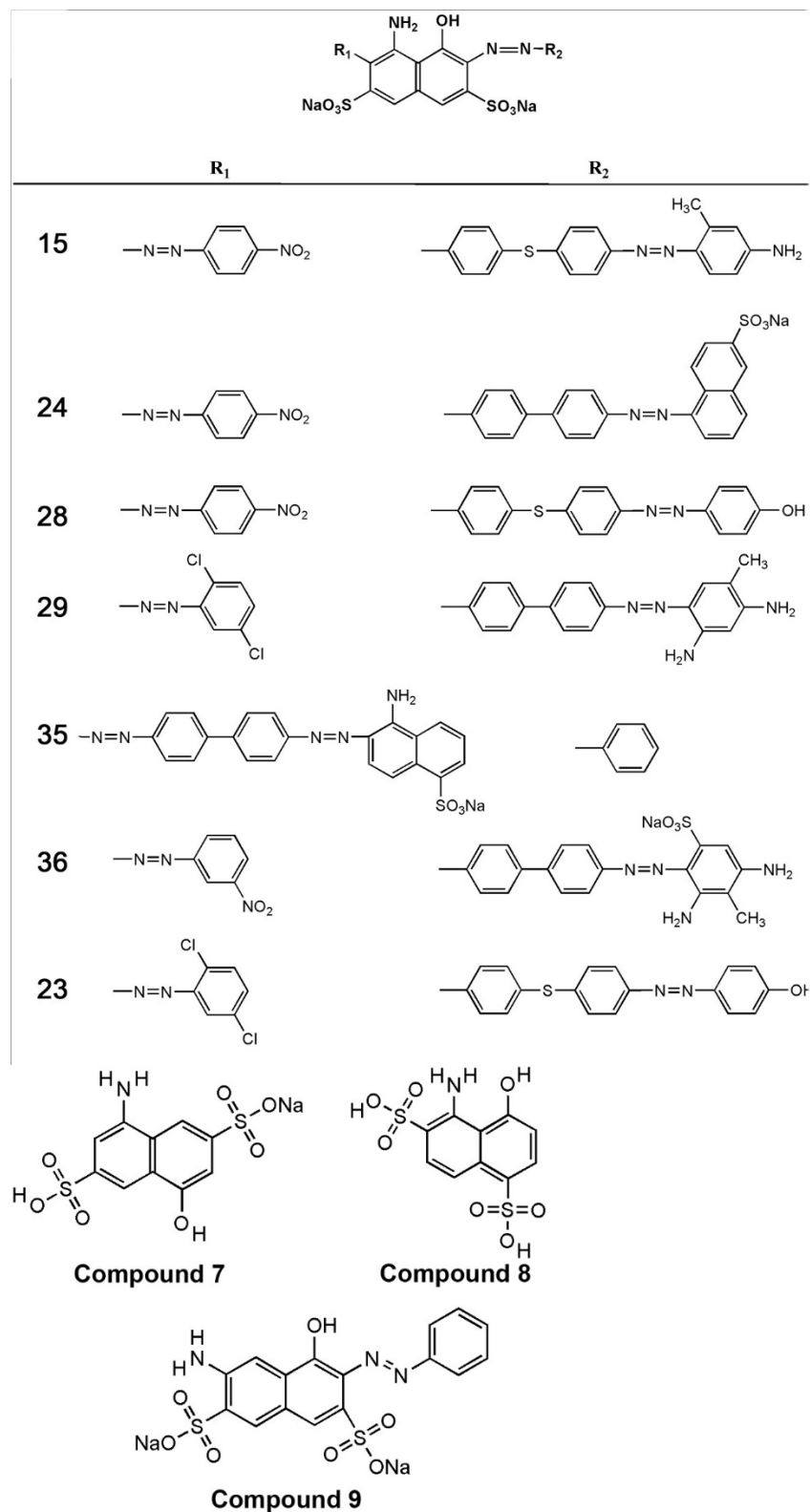
Sean Jmaeff, Yulia Sidorova, Hayley Lippiatt, Pablo F. Barcelona, Hinyu Nedev, Lucia M. Saragovi, Mark A. Hancock, Mart Saarma, H. Uri Saragovi

Compound	MG87 RET/GFR α 1		MG87 RET	
	5 μ M	20 μ M	5 μ M	20 μ M
116	102.3124	134.8646	99.44444	117.8862
206	162.1520	122.5338	121.6667	102.0325
210	268.2869	265.0870	133.3333	121.1382
302	121.7084	180.3675	102.7778	105.2846
226	262.9070	227.1760	182.7778	163.4146
224	131.9018	247.6306	99.44444	111.7886
65	162.0104	230.2708	130.5556	174.3902
47	136.6210	166.2476	140.0000	180.4878
29	258.9429	330.0290	185.0000	252.0325

Supplemental Table 1. Initial Compound Screening. In initial screens, ~200 compounds were tested in MG87 cells with and without GFR α 1 expression at 5 and 20 μ M. Data from a select panel are shown as the average relative increase in luminescence versus vehicle from 4 experiments. **Compound 29** was selected as a candidate hit as it generated significant increases in both cell types, and subsequent analogues were then tested. In these assays, GDNF as positive control induces higher increases in luciferase activity, ranging from 60-80 fold over vehicle, consistent with previous reports (Sidorova et al, 2010).

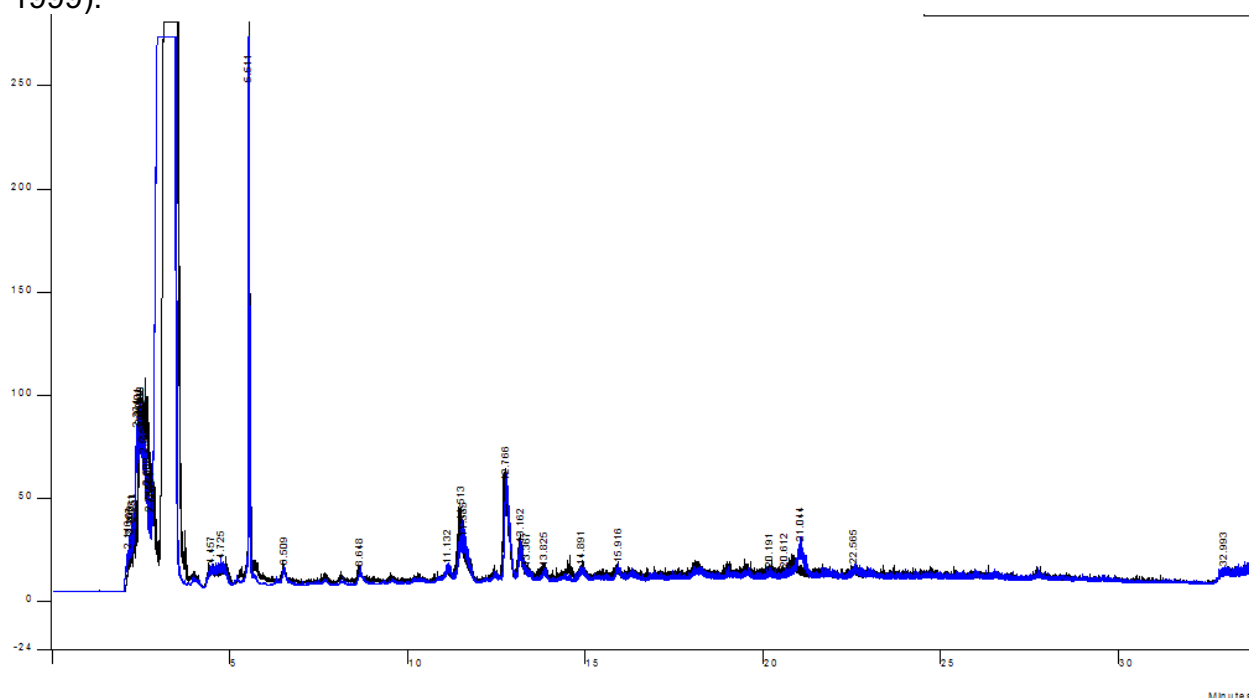
Supplemental Figure 1.

Compound Structures. Overview of the structures as they are described by the NCI.



Structural Properties of NCI Database Compounds and 4-amino-5-hydroxynaphthalene-1,3-disulfonic Acid

4-amino-5-hydroxynaphthalene-1,3-disulfonic acid was obtained commercially from TCI America (Product Code: A0363) as a dark powder with reported purity of >85.0%. Both Compound 8 and this product were purified on a 250 mm x 10 mm Kromasil 100-5-C18 semi-preparative column. A solvent gradient of 5-30%B was used for 30 minutes, where solvent A was HPLC grade H₂O with 0.1% TFA, and solvent B was a 70/30 mix of Acetonitrile/H₂O with 0.1% TFA. Samples of each were lyophilized yielding an off-white powder and dissolved in D₂O for subsequent ¹H-NMR at 500 MHz. ESI mass spectra were obtained in negative mode with a Bruker Maxis Impact. Compounds 15, 23, 29, and 35 were dissolved in DMSO for mass spec analysis. Sulfonic acids ionize preferentially in negative mode, and commonly yield di-charged ions by ESI (Holcapek 1999).



Supplemental Figure 2. HPLC chromatogram of the 5-30%B gradient showing 2 mg injections of 4-amino-5-hydroxynaphthalene-1,3-disulfonic Acid (Blue) and Compound 8 (Black). Both were relatively pure with the major fraction eluting ~3min. The overlay of the chromatograms suggest that the impurities in the mixture are likely to be similar.

Supplemental Figure 3.

H-NMR resonances and the detected mass of 4-amino-5-hydroxynaphthalene-1,3-disulfonic Acid and of Compound 8 show that they are likely the same molecule.

Therefore compound 8 is incorrectly identified in the NCI database. Other agents (compounds 15,23,29,35) are also shown, and they correspond to the NCI-reports.

Compound 8 (NSC37052). ¹H-NMR (D₂O, 500 MHz): δ 8.17 (s, 1H), 7.90 (dd, J = 8.6, 0.9 Hz, 1H), 7.44 – 7.37 (t, 1H), 6.84 (dd, J = 7.8, 0.9 Hz, 1H).

MS (ESI,-) *m/z* calcd for C₁₀H₇NO₇S₂ [M-2H]²⁻ calcd: 158.4837, found: 158.4841

4-amino-5-hydroxynaphthalene-1,3-disulfonic acid. ¹H-NMR (D₂O, 500 MHz): δ 8.16 (s, 1H), 7.89 (dd, J = 8.5, 1.0 Hz, 1H), 7.44 – 7.37 (t, 1H), 6.84 (dd, J = 7.8, 1.1 Hz, 1H). MS (ESI,-) *m/z* calcd for C₁₀H₇NO₇S₂ [M-2H]²⁻ calcd: 158.4837, found: 158.4840

Compound 15 (NSC65571). MS (ESI,-) *m/z* calcd for C₃₅H₂₅N₉O₉S₃ [M-2H]²⁻ calcd: 405.5474, found: 405.5460

Compound 23 (NSC75661). MS (ESI,-) *m/z* calcd for C₃₄H₂₁Cl₂N₇O₈S₃ [M-2H]²⁻ calcd: 410.5001, found: 410.5009

Compound 29 (NSC79730). MS (ESI,-) *m/z* calcd for C₃₅H₂₅Cl₂N₉O₇S₂ [M-2H]²⁻ calcd: 408.5353, found: 408.5356

Compound 35 (NSC79745). MS (ESI,-) *m/z* calcd for C₃₈H₂₅N₈NaO₁₀S₃ [M-2H]²⁻ calcd: 436.0382, found: 436.0397

